Int. J. Electrochem. Sci., 6 **(2011)** 1479 - 1492

International Journal of
ELECTROCHEMICAL
SCIENCE
www.electrochemsci.org

Corrosion and Corrosion Inhibition of Aluminum in Arabian Gulf Seawater and Sodium Chloride Solutions by 3-Amino-5-Mercapto-1,2,4-Triazole

El-Sayed M. Sherif [1,2,*]

[1] Center of Excellence for Research in Engineering Materials (CEREM), College of Engineering, King Saud University, P. O. Box 800, Al-Riyadh 11421, Saudi Arabia
[2] Electrochemistry and Corrosion Laboratory, Department of Physical Chemistry, National Research Centre (NRC), Dokki, 12622 Cairo, Egypt
[*]E-mail: esherif@ksu.edu.sa

Received: 12 March 2011 / *Accepted:* 28 April 2011 / *Published:* 1 May 2011

Corrosion of aluminum in aerated Arabian Gulf seawater (AGS) and 3.5% NaCl solutions and its inhibition by 3-amino-5-mercapto-1,2,4-triazole (AMTA) have been reported. The study was carried out using cyclic potentiodynamic polarization (CPP), current-time at constant potential (CT), and electrochemical impedance spectroscopy (EIS) measurements. Experimental results indicated that the presence of AMTA molecules inhibit the general and pitting corrosion of Al in both AGS and NaCl solutions by shifting the corrosion and pitting potentials of Al to the more noble values, decreasing the corrosion and passivation currents and corrosion rate, while increasing the surface and charge transfer resistances. This effect was remarkably increased by increasing the AMTA concentration to $5x10^{-3}$ M. Although, AGS showed more aggressiveness towards Al than 3.5% NaCl, the inhibition efficiency of AMTA is higher for Al in AGS solution. The inhibition of Al corrosion by AMTA molecules is achieved by their adsorption then formation of a complex with the aluminum oxide preventing the formation of aluminum chlorides, $AlCl_3$, or chloride complexes, $AlCl_4^-$ or even soluble oxychloride complexes, $Al(OH)_2Cl_2^-$, which lead to Al corrosion.

Keywords: Aluminum corrosion, Arabian Gulf seawater, 3-amino-5-mercapto-1,2,4-triazole, corrosion inhibitors, electrochemical measurements, sodium chloride solutions

1. INTRODUCTION

Aluminum is an important metal in industry owing to its many excellent characteristics including its good electrical and thermal conductivities, low density, high ductility, and good corrosion resistance. It is widely used as a material for automobiles, aviation, household appliances, containers,

and electronic devices [1, 2]. The corrosion resistance of aluminum arises from its ability to form a natural oxide film on its surface in a wide variety of media [2–4]. This oxide film can readily undergo corrosion reactions as has been reported in many investigations into the electrochemical behavior and corrosion resistance of aluminum in different environments and especially containing chloride ions [1–6].

Seawater is a complex mixture of inorganic salts, dissolved gases, suspended solids, organic matter and organisms [7]. Arabian Gulf seawater (AGS) has inorganic salts that include Na^+, Mg^{2+}, K^+, Ca^{2+}, and Sr^{2+} as well as very high concentrations of chloride (24090 mg/L), and sulfate (3384 mg/L) ions. AGS also has HCO_3^-, Br-, and F^-, with total dissolved solids (TDS) of 43800 mg/L [7]. The presence of such high TDS concentration represents a very corrosive medium. It has been reported [1, 2, 8] also that the high concentration of NaCl (3.5% NaCl) simulates the sea water environment.

Protective oxide films formed on the aluminum surface have a dual nature. These films consist of an adherent, compact, and stable inner oxide film covered with a porous, less stable outer layer, which is more susceptible to corrosion [9–11]. It is generally believed that the dissolution of aluminum oxide films, which leads to the corrosion of aluminum, results from the adsorption of chloride ions that react with aluminum cations in the oxide lattice, leading to the formation of a soluble aluminum hydroxychloride salt. This salt goes into solution allowing the films to dissolve, leaving the bare aluminum metal [12, 13]. According to Hunkeler et al. [14] and Sato [15], a salt barrier of $AlCl_3$ is formed within the pits on their formation and converted to soluble $AlCl_4^-$, which diffuses into the bulk solution.

The protection of aluminum and its oxide films from the corrosive chloride attack has been studied by many investigators using either inorganic oxidants including chromate [11, 16, 17], molybdate [16–18], and tungstate [16, 19], organic compounds having polar groups, such as oxygen, sulfur, and nitrogen [1, 2, 20–22], and heterocyclic compounds containing functional groups and conjugated double bonds [23] as corrosion inhibitors. It has been reported [24] that the inhibitor molecules are bonded to the metal surface by chemisorption, physisorption, or complexation with the polar groups acting as the reactive centers in the molecules. In general, the adsorption of an inhibitor on a metal surface depends on a few factors [1, 2], such as the nature and surface charge of the metal, the adsorption mode, the inhibitor's chemical structure, and the type of the electrolyte.

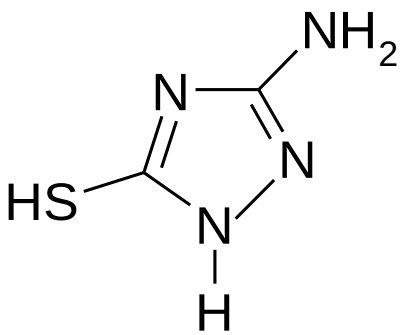

Scheme1. Chemical structure of 3-amino-5-mercapto-1,2,4-triazole (AMTA)

In our previous work, the effect of 1,5-naphthalenediol [1] and 1,4-naphthoquinone [2] on Al corrosion in 0.5 M NaCl has been reported. Yamaguchi and Yamamoto [25] also investigated the adsorption of poly(1,5-naphthalenediol) on Al surface. In all these studies, the organic compounds have proven strong ability to be adsorbed then to form a complex with Al surface by the formation of the Al-O bond, which lead to the inhibition of Al corrosion. The objective of the present work is to report the effect of 3-amino-5-mercapto-1,2,4-triazole (AMTA, scheme 1) on the inhibition of Al corrosion in both Arabian Gulf seawater (AGS) and 3.5% sodium chloride solutions using different electrochemical techniques. Azole derivatives have been reported to inhibit the corrosion of different metals such as copper, iron, etc. [25–28]. AMTA is nontoxic and inexpensive and was expected to inhibit the corrosion of Al in AGS and chloride solutions because it is a heterocyclic compound containing different donor atoms.

2. EXPERIMENTAL PROCEDURE

2.1. Chemicals and electrochemical cell

3-Amino-5-mercapto-1,2,4-triazole (AMTA, Sigma–Aldrich, 95%), sodium chloride (NaCl, Merck, 99%), natural seawater (AGS) was obtained directly from the Arabian Gulf at the eastern region (Jubail, Dammam, Saudi Arabia), and N,N-dimethylfomamide ((formdimethylamide), was purchased from WinLab, Wilfrid Smith Limited (Middlesex, UK)) were used as received. An electrochemical cell with a three-electrode configuration was used; an aluminum rod (Al, Aldrich, 99.99%, 6.5 mm in diameter), a platinum foil, and an Ag/AgCl electrode (in the saturated KCl) were used as the working, counter, and reference electrodes, respectively. The Al rod for electrochemical measurements was prepared by welding a copper wire to a drilled hole was made on one face of the rod; the rod with the attached wire were then cold mounted in resin and left to dry in air for 24 h at room temperature. Before measurements, the other face of the Al electrode, which was not drilled, was first grinded successively with metallographic emery paper of increasing fineness up to 800 grit and further polished with 5, 1, 0.5, and 0.3 mm alumina slurries (Buehler). The electrode was then cleaned using doubly-distilled water, degreased with acetone, washed using doubly-distilled water again and finally dried with dry air.

2.2. Electrochemical methods

Electrochemical experiments were performed by using an Autolab Potentiostat (PGSTAT20 computer controlled) operated by the general purpose electrochemical software (GPES) version 4.9. The cyclic polarization curves (CPP curves were obtained by scanning the potential in the forward direction from -1800 to -500 mV against Ag/AgCl at a scan rate of 3.0mV/s; the potential was then reversed in the backward direction at the same scan rate. Chronoamperometric current-time (CT) experiments were carried out by stepping the potential of the aluminum samples at – 680 mV versus Ag/AgCl for 60 minutes. Impedance (EIS) tests were performed at corrosion potentials (E_{Corr}) over a

frequency range of 100 kHz – 100 mHz, with an ac wave of ± 5 mV peak-to-peak overlaid on a dc bias potential, and the impedance data were collected using Powersine software at a rate of 10 points per decade change in frequency. All the electrochemical experiments were carried out at room temperature in freely aerated solutions.

3. RESULTS AND DISCUSSION

3.1. Cyclic potentiodynamic polarization (CPP) data

The CPP curves obtained for an Al electrode after 1 h immersion in of (1) AGS and (2) 3.5% NaCl solutions are shown in Fig. 1. The cathodic reaction for aluminum in aerated near neutral pH solutions has been reported [7, 8] to be the oxygen reduction as follows;

$$\frac{1}{2}O_2 + H_2O_{(S)} + e^- = OH_{ads.} + OH^- \qquad (1)$$

The adsorbed hydroxide species further reduced to be in the solution accordingly;

$$OH_{ads.} + e^- = OH^- \qquad (2)$$

It is seen from Fig. 1 that the corrosion potential (E_{Corr}) of Al in the aerated solution of AGS (curve 1), recorded −1435 mV vs.

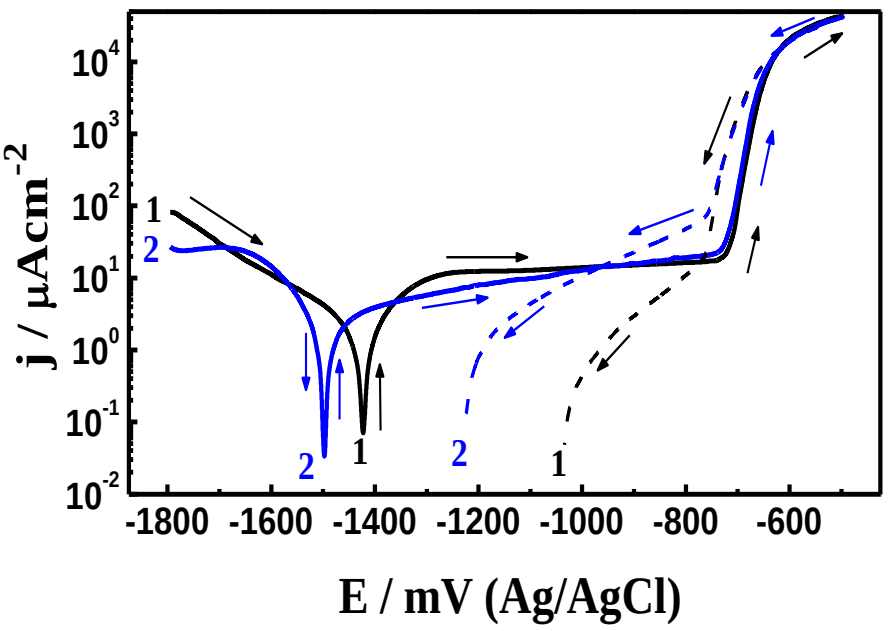

Figure 1. CPP curves obtained for Al electrode after its immersion for 1 h in (1) AGS and (2) 3.5% NaCl solutions.

Ag/AgCl and a corrosion current density (j_{Corr}) of 2.5 µA cm^{-2} with a wide passive region with its average current density of ~ 4.8 µAcm^{-2}, extending from −1350 to −740 mV due to the formation of an oxide film on the aluminum electrode surface. This film is formed by the anodic reaction on two steps as follows [1, 2];

$$Al_{(S.)ads.} + 3OH^- = Al(OH)_{3,ads.} + 3e^- \quad (3)$$

Then this aluminum hydroxide, $Al(OH)_{3,ads.}$, transforms to the aluminum oxide, $Al_2O_3 \cdot 3H_2O$,

$$2Al(OH)_{3,ads.} = Al_2O_3 \cdot 3H_2O \quad (4)$$

The breakdown of the passive film took place due to the occurrence of pitting corrosion under the influence of the negative applied potential and presence of aggressive species such as chloride ions in the AGS medium [1, 2, 7]. This was indicated by the abrupt increase in the current values at less negative potential than −738 mV and can be explained by these reactions;

$$Al = Al^{3+} + 3e^- \quad (5)$$

And

$$Al^{3+} + 4Cl^- = AlCl_4^- \quad (6)$$

There are some opinions regarding the mechanism of pitting corrosion of Al in chloride containing solutions [12−15]. One claims that a salt barrier of $AlCl_3$ is formed within the pits on their formation to form $AlCl_4^-$ as shown in Eq. (6), which diffuses into the bulk of the solution allowing the pitting corrosion to occur. Another view suggests the aggressiveness of the chloride ions is ascribed to their adsorption and their reaction with Al(III) in the oxide lattice, which leads to the formation of oxychloride complexes, $Al(OH)_2Cl_2^-$;

$$Al^{3+}_{(\text{in crystal lattice of the oxide})} + 2Cl^- + 2OH^- = Al(OH)_2Cl_2^- \quad (7)$$

The formation of $Al(OH)_2Cl_2^-$ as a soluble complex decreases the chemical inertness of the natural oxide film and consequently enhances the anodic dissolution of the Al metal.

The CPP curve of Al in 3.5% NaCl (Fig. 1, curve 2) shows similar behavior with more negative shift in E_{Corr} recording −1485 mV and a lower value of j_{Corr}, 2.0 µA cm^{-2}. Also, the average passive current density recorded lower value ~ 4.5 µAcm^{-2}, with wider passive region extending from −1440 to −710 mV. The values of E_{Corr}, j_{Corr}, cathodic Tafel slope (βc), anodic Tafel slope (βa), passivation current (j_{Pass}), pitting potential (E_{Pit}), polarization resistance (R_P), and corrosion rate (K_{Corr}) for Al after its immersion in AGS and 3.5% NaCl solutions for 1 h obtained from the polarization curves shown in Fig. 1 are listed in Table 1. The values of the E_{Corr} and j_{Corr} were obtained from the extrapolation of anodic and cathodic Tafel lines located next to the linearized current regions. The j_{Pit} was determined from the forward anodic polarization curves where a stable increase in the current density occurs. The values of K_{Corr} and R_P were calculated as reported in our previous work [8, 29–37]. Fig. 1 and Table 1

indicate that AGS is slightly more aggressive than 3.5% NaCl solution towards aluminum, where the values of j_{Corr}, cathodic, anodic, and j_{Pass} currents and K_{Corr} are higher, while the value of R_P is lower.

Table 1. Corrosion parameters obtained from cyclic potentiodynamic polarization curves shown in Fig. 1 and Fig. 2 for the Al electrode in AGS and 3.5% NaCl solutions in absence and presence of AMTA.

Solution	Parameter								
	E_{Corr} / mV	j_{Corr} / µA cm^{-2}	B_c / mV dec^{-1}	B_a / mV dec^{-1}	j_{Pass} / µA cm^{-2}	E_{Pit} / mV	R_p / Ω cm^2	K_{Corr} / mmy^{-1}	IE / %
AGS only	-1435	2.5	180	170	4.83	-738	15.22	0.0273	─
+ 10^{-3} M AMTA	-1375	0.5	135	195	3.65	-710	69.38	0.0055	79.8
+ 5x10^{-3} M AMTA	-1340	0.35	105	210	1.28	-685	86.95	0.0038	86.1
3.5% NaCl only	-1485	2.0	140	165	4.52	-735	16.46	0.0218	─
+ 10^{-3} M AMTA	-1395	0.6	105	180	3.14	-725	48.10	0.0065	70.2
+ 5x10^{-3} M AMTA	-1355	0.42	92	207	1.49	-690	65.93	0.0046	78.9

Fig. 2 shows the CPP curves of Al electrode after its immersion for 1 h in solutions of (a) AGS in absence (1) and presence of 10^{-3} M AMTA (2) and 5x10^{-3} M AMTA (3); and (b) 3.5% NaCl in absence (1) and presence of 10^{-3} M AMTA (2) and 5x10^{-3} M AMTA (3). The corrosion parameters and the percentage of the inhibition efficiency (*IE %*) obtained from Fig. 2 are listed in Table 1. The presence of 10^{-3} M AMTA in the test solutions (curves 2) shifts both the E_{Corr} and E_{Pit} to more positive potential values. Also, the values of j_{Corr}, j_{Pass} and K_{Corr} decrease, while the R_P values increase. More noble corrosion and pitting potentials with lower corrosion current, passivation current, and corrosion rate were recorded up on the increase of AMTA concentration to 5x10^{-3} M. The positive shift in E_{Corr} values in the presence of AMTA indicates that AMTA molecules adsorb on the surface and prevent the $Al(OH)_2Cl_2^-$, (*see Eq. 7*), from being formed on the oxide film and thus decrease the aggressiveness of Cl─ as well as protect the surface from being pitted. This suggests that the AMTA inhibits the corrosion of Al in both AGS and 3.5% NaCl solutions and its efficiency as a corrosion inhibitor increases with the increase of its content in the solution. The calculated values of *IE%* (Table 1) recorded higher values in AGS (80% and 86% for 1x10^{-3} and 5x10^{-3} M AMTA, respectively) than those in 3.5% NaCl solutions (70% and 80%, respectively) at the same AMTA concentration. This reveals that AMTA molecules are more powerful in protecting the corrosion of Al in AGS than 3.5% NaCl solution. According to our previous studies [1, 2], the corrosion inhibition of Al at this condition is obtained by either the adsorption of AMTA onto the aluminum surface blocking the corrosion process by repairing the flawed area on the surface in a way similar to the case of sodium benzoate and phosphate [38].

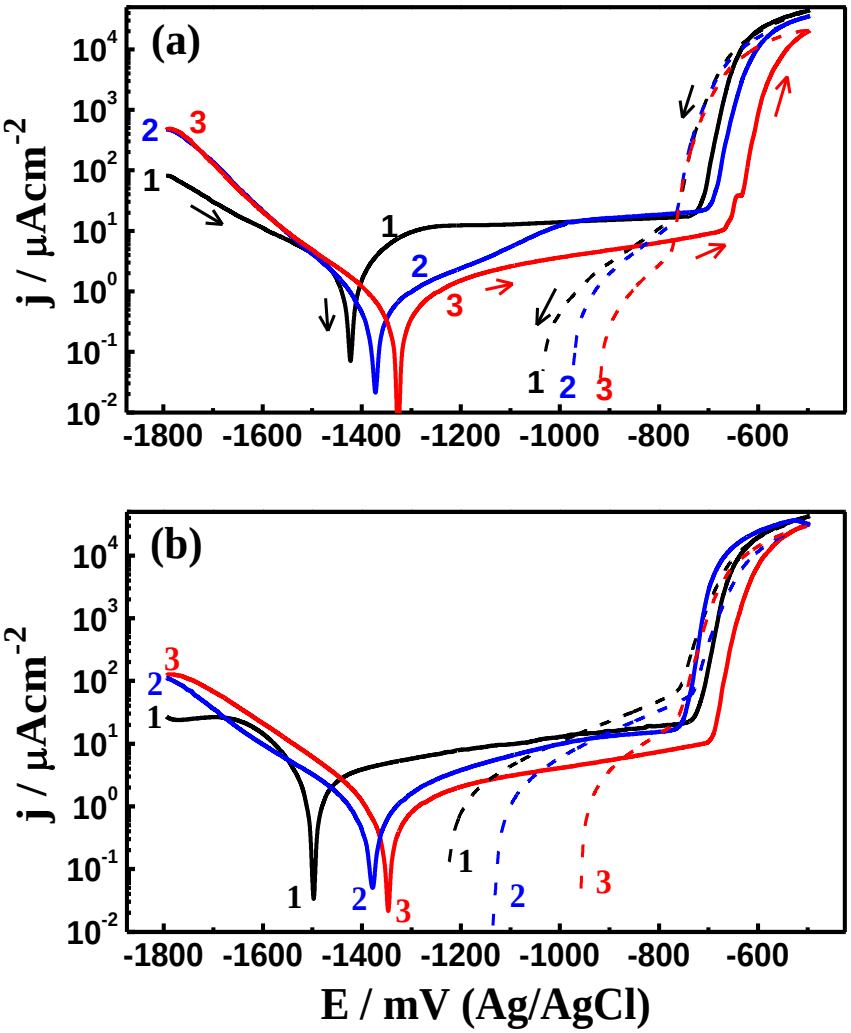

Figure 2. CPP curves obtained for Al electrode after its immersion for 1 h in solutions of: **(a)** AGS in absence (1) and presence of $1x10^{-3}$ M AMTA (2) and $5x10^{-3}$ M AMTA (3); and **(b)** 3.5% NaCl in absence (1) and presence of $1x10^{-3}$ M AMTA (2) and $5x10^{-3}$ M AMTA (3).

3.2. Chronoamperometric current-time measurements

In order to shed more light on the corrosion and corrosion inhibition of aluminum in AGS and NaCl solutions in absence and presence of AMTA at less negative potentials, potentiostatic current–time experiments were carried out. The chronoamperometric curves obtained at –680 mV (Ag/AgCl) for Al electrode after its immersion for 1 h in (1) AGS and (2) 3.5% NaCl solutions are shown in Fig. 3. It is noted from Fig. 3 that currents increased in the first few moments of stepping the potential in both AGS and NaCl solutions. This is due to the dissolution the oxide film that was formed during the immersion of Al in the test solution and before applying the active potential. The currents then decreased rapidly during the first 10 min as a result of stabilizing an oxide film and/or corrosion product layer on the electrode surface. Again, a further slow decrease in currents with small fluctuations is observed with increasing the time till the end of the run due to the thickening of Al_2O_3 and/or the accumulation of corrosion products. This current-time behavior indicates that AGS is more

aggressive than 3.5% NaCl on Al surface because the absolute current in the chloride solution is lower than that for the seawater, which agrees with the CPP experimental data.

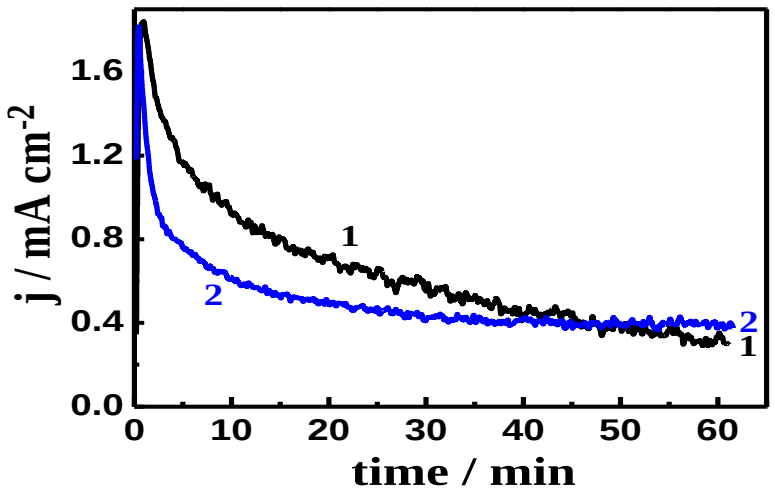

Figure 3. Chronoamperometric current-time curves obtained at –680 mV (Ag/AgCl) for Al electrode after its immersion for 1 h in (1) AGS and (2) 3.5% NaCl solutions.

Fig. 4a depicts the current-time curves obtained for Al electrode at –680 mV (Ag/AgCl) after its immersion for 1 h in AGS solutions containing (1) 0 AMTA, (2) 10^{-3} M ATMA and (3) $5x10^{-3}$ M AMTA. The current-time of Al in AGS with the presence of 10^{-3} M AMTA shows similar behavior to that in the absence of AMTA but with lower absolute current values along the whole time of the experiment. More decreases of currents were recorded with increasing time, where the value of current of Al after 1 h of applying –680 mV in AGS only was 315 μA cm^{-2} decreased to 112 μA cm^{-2}. This indicates that the AMTA at this concentration does not change the mechanism of Al dissolution or passivation but enhances the formation of Al_2O_3. Increasing the concentration of AMTA to $5x10^{-3}$ (Fig. 4a, curve 3) lowered the currents of Al from the start of the run and increased slightly in the first 25 min after which, it decreased with time again to record 86 μA cm^{-2} after 1h of applying the constant potential.

Chronoamperometric current-time curves obtained for Al at –680 mV after its immersion for 1 h in 3.5% NaCl in absence (1) and presence of 10^{-3} M AMTA (2) and $5x10^{-3}$ M AMTA (3) are shown in Fig. 4. The presence of AMTA with chloride solution decreased the absolute currents of Al from the first moment till the end of the measurement. Further pronounced decreasing of currents was obtained with increasing the AMTA concentration to $5x10^{-3}$, curve 3. It clearly seen from Fig. 4 that AMTA inhibited the dissolution of Al in both AGS and chloride solutions and its efficiency as an inhibitor was higher in AGS than in 3.5% NaCl, which agrees with the polarization data shown in Fig. 2. It has been reported that [1, 2, 25] that organic compounds inhibit Al corrosion via their adsorption then form a complex leading to the formation of Al-O bond, which preclude Al dissolution. This explains the decrease of current values with time in the presence of AMTA molecules in the test solution.

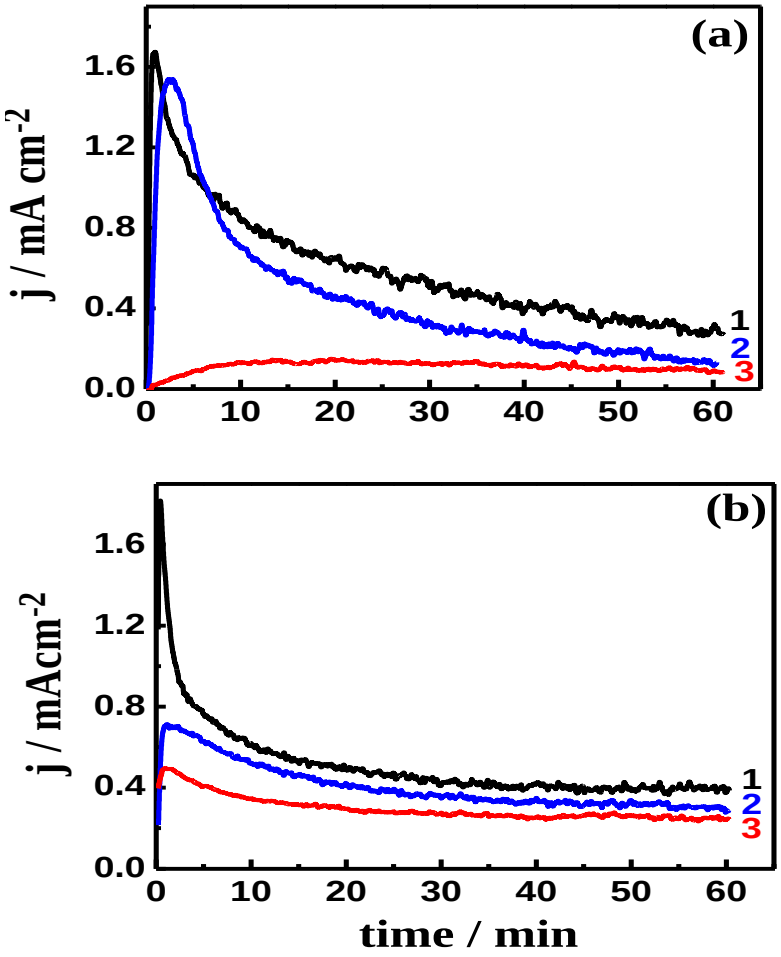

Figure 4. Chronoamperometric current-time curves obtained at –680 mV (Ag/AgCl) for Al electrode after 1 h exposure in solutions of: **(a)** AGS without (1) and with $1x10^{-3}$ M AMTA (2) and $5x10^{-3}$ M AMTA (3); and **(b)** 3.5% NaCl without (1) and with $1x10^{-3}$ M AMTA (2) and $5x10^{-3}$ M AMTA (3).

3.3. Electrochemical impedance spectroscopy (EIS) measurements

EIS provides important mechanistic and kinetic information for corrosion and corrosion inhibition of metals and alloys in corrosive media [29–37, 39–44]. The EIS measurements in this study were carried out in order to determine the impedance characteristics at the aluminum/electrolyte interface and to confirm the data obtained by polarization and current-time experiments. EIS Nyquist plots obtained at an open-circuit potential for Al electrode after 1 h of exposure to (1) AGS and (2) 3.5% NaCl solutions are represented in Fig. 5. Nyquist plots were also obtained at the same condition in the absence (1) and the presence of $1x10^{-3}$ M AMTA (2), and $5x10^{-3}$ M AMTA (3) for Al electrode after its exposure for 1 h in AGS and 3.5% NaCl solutions and the data are shown in Fig. 6a and Fig. 6b, respectively. It is clear from Fig. 5 and Fig. 6 that only single semicircles are observed for the Al electrode in AGS and NaCl solutions regardless of whether AMTA is present or not. The chord length pertaining to the high frequency (HF) loop observed in Nyquist diagram related to AGS (Fig. 5, curve 1) is smaller than the corresponding one in case of NaCl solution (curve 2). The increase of the HF

chord recorded for Al in NaCl solution is perhaps due to the decrease in the electrochemical active and flawed areas either by the thickening of Al_2O_3 (Eq. 4) or by the accumulation of other insoluble corrosion products with the oxide at the Al surface. The diameter of the semicircle is noticed to increase in the presence of AMTA and up on the increase of its concentration as depicted in Fig. 6. It has been reported that the semicircles at high frequencies are generally associated with the relaxation of the capacitors of electrical double layers with their diameters representing the charge transfer resistances [1, 26, 36, 45].

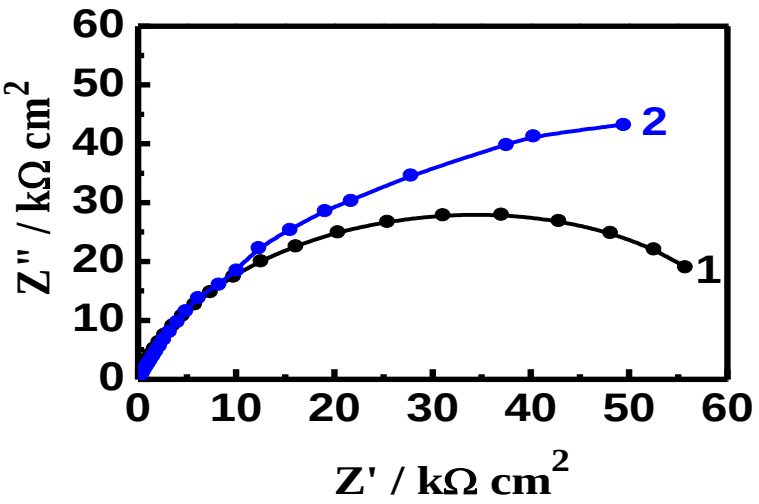

Figure 5. EIS Nyquist plots for Al electrode at an open-circuit potential after its exposure for 1 h in (1) AGS and (2) 3.5% NaCl solutions.

Table 2. EIS parameters obtained by fitting the Nyquist plots shown in Fig. 5 and Fig. 6 with the equivalent circuit shown in Fig. 7 for the aluminum electrode in AGS and 3.5% NaCl solutions.

Parameter									
		Q_1				Q_2			
Solution	R_S / Ωcm^2	Y_{Q1} / μF cm^{-2}	n	R_{P1} / kΩcm^2	W / Ω S$^{-1/2}$	Y_{Q2} / μF cm^{-2}	n	R_{P2} / kΩcm^2	IE / %
AGS only	0.01	8.37	0.88	9.94	21x10^{-6}	0.441	1.0	13.98	–
+ 10^{-3} M AMTA	0.01	9.768	0.84	41.82	6.1x10^{-6}	0.317	0.80	17.53	76.2
+ 5x10^{-3} M AMTA	19.1	9.073	0.83	59.97	4.1x10^{-6}	0.122	0.84	22.2	83.4
3.5% NaCl only	1E-7	11.62	0.81	10.58	4.8x10^{-5}	0.392	1.0	14.89	–
+ 10^{-3} M AMTA	14.33	11.04	0.87	37.14	6.7x10^{-6}	0.298	0.58	19.15	71.7
+ 5x10^{-3} M AMTA	21.81	11.03	0.89	52.17	5.4x10^{-6}	0.167	0.68	24.3	79.8

In order to better understand the EIS data, the impedance spectra shown in Fig. 5 and Fig. 6 were analyzed by fitting it to the equivalent circuit model shown in Fig. 7. This circuit was used before in the fitting of EIS data obtained in studying the inhibition of aluminum corrosion sodium chloride solutions using different concentrations of 1,5-naphthalenediol as a corrosion inhibitor [1]. The EIS parameters obtained by fitting the equivalent circuit shown in Fig. 7 are listed in Table 2. According to usual convention, R_S represents the solution resistance, Q_1 the constant phase elements (CPEs), Q_2 another constant phase elements, R_{P1} the polarization resistance and can be defined as the charge transfer resistance of the oxygen reduction reaction (see reaction (1)) [45], R_{P2} another polarization resistance, and *W* the Warburg impedance.

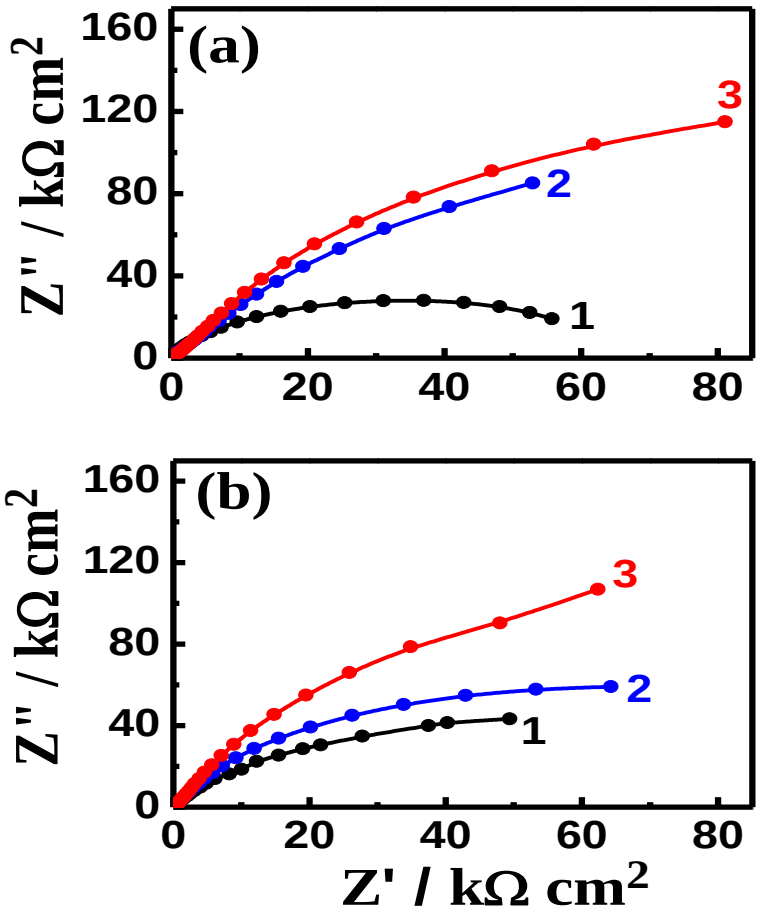

Figure 6. Typical Nyquist plots for Al electrode at corrosion potential after 1 h immersion in: **(a)** AGS solutions, (1) without, (2) with $1x10^{-3}$ M AMTA, and (3) $5x10^{-3}$ M AMTA; and **(b)** 3.5% NaCl solutions, (1) without, (2) with $1x10^{-3}$ M AMTA, and (3) $5x10^{-3}$ M AMTA.

It is clearly noted from Fig. 6 and Table 2 that R_S, R_{P1} and R_{P2} for Al in 3.5% NaCl solutions are higher than that ones in AGS confirming that AGS is more aggressive towards Al than 3.5% NaCl, which is in good agreement with the data obtained by polarization and current-time measurements. The surface and polarization resistances also increase in the presence of AMTA and up on the increase of its concentration indicating that the surface is more corrosion resistant. This is also in general

agreement with the positive shift in the pitting and corrosion potentials. The constant phase elements (CPEs), Q_1 and Q_2 with their *n*-values equal 1.0 or close to 1.0 represent double layer capacitors with porous structures on the surface. The decrease of the CPEs especially in presence of AMTA and the increase of its content suggests that the charged surfaces are covered with an adsorbed layer of AMTA, which is expected to reduce the pore densities leading to the reduction in capacitive effects. The presence of the Warburg (*W*) impedance limits the surface reaction by mass transport.

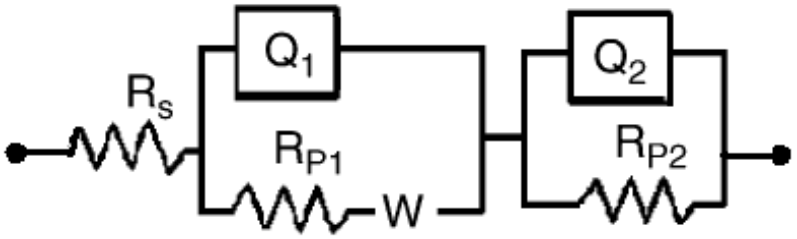

Figure 7. The equivalent circuit used to fit the experimental data presented in Fig. 6.

The *IE%* of AMTA for the aluminum electrode can be then calculated from the charge transfer resistance as follows [33-35],

$$IE\% = \frac{R_{P1} - R_{P1}^{-}}{R_{P1}} \qquad (8)$$

Where R_{P1} and R_{P1}^{-} are the charge transfer resistances with and without AMTA present, respectively; the values of the calculated *IE%* are also listed in Table 2. The value of *IE%* obtained for Al in AGS solutions by 10^{-3} M AMTA was circa 76% increased to 83% when the concentration of AMTA increased to $5x10^{-3}$M. These values of *IE%* decreased to about 72% and 80% at the same ATMA concentration, respectively for Al in 3.5% NaCl solutions. This confirms the results obtained by CPP and CT data and also proves that AMTA is more efficient in precluding the corrosion of Al in AGS than 3.5% NaCl and its ability as a corrosion inhibitor increases with increasing its concentration.

4. CONCLUSIONS

Corrosion of aluminum in aerated Arabian Gulf seawater (AGS) and 3.5% NaCl solutions and its inhibition by 3-amino-5-mercapto-1,2,4-triazole (AMTA) have been studied. CPP measurements for Al in AGS and NaCl solutions showed that AGS is more corrosive. CPP tests indicated also that the presence of AMTA molecules and the increase of its concentration shift the corrosion and pitting potential of Al towards the less negative values and decrease anodic, corrosion, cathodic, passivation and pitting currents and the corrosion rate as well as increase the polarization resistance. CT

experiments revealed that AMTA decreases the absolute currents of Al in both AGS and NaCl solutions and this effect increases with increasing AMTA concentration. EIS data confirmed that one's obtained by CPP and CT and proved that the surface and polarization resistances increase in the presence and up on the increase of AMTA concentration. The values of *IE%* for 10^{-3} M AMTA obtained by CPP and EIS recorded an average of ~ 78% and 70% increased to about 84% and 79% with $5x10^{-3}$ in AGS and NaCl solutions, respectively. AMTA as an inhibitor works by adsorption onto aluminum preventing its corrosion by preventing the formation of soluble chloride and oxychloride complexes on its surface. Results collectively are in good agreement and show clearly that AGS is more corrosive than 3.5% NaCl and AMTA is a good corrosion inhibitor for Al and its efficiency is higher for AGS than 3.5% NaCl solutions.

ACKNOWLEDGEMENTS
The author extend his appreciation to the Deanship of Scientific Research at KSU for funding the work through the research group project No. RGP-VPP-160.

References

1. E. M. Sherif, S.-M. Park, *Electrochim. Acta*, 51 (2006) 1313.
2. E. M. Sherif, S.-M. Park, *J. Electrochem. Soc.*, 152 (2005) B205.
3. W. R. Osório, N. Cheung, L. C. Peixoto, A. Garcia, *Int. J. Electrochem. Sci.*, 4 (2009) 820.
4. W. Diggle, T. C. Downie, C. Goulding, *Electrochim. Acta*, 15 (1970) 1079.
5. Fang Wang, Yabin Wang, Yanni Li, *Int. J. Electrochem. Sci.*, 6 (2011) 793.
6. A. I. Onen, B. T. Nwufo, E. E. Ebenso, R. M. Hlophe, *Int. J. Electrochem. Sci.*, 5 (2010) 1563.
7. A. M. Shams El Din, M. E. El Dahshan, A. M. Taj El Din, Desalination 130 (2000) 89.
8. E. M. Sherif, R. M. Erasmus, J. D. Comins, *J. Colloid Inter. Sci.*, 309 (2007) 470.
9. G. A. Capauano, W. G. Davenport, *J. Electrochem. Soc.*, 118 (1971) 1688.
10. I. B. Obot, N. O. Obi-Egbedi, S. A. Umoren, *Int. J. Electrochem. Sci.*, 4 (2009) 863.
11. C. M. A. Brett, I. A. R. Gomes, J. P. S. Martins, *Corros. Sci.*, 36 (1994) 915.
12. R. T. Foley, T. H. Nguyen, *J. Electrochem. Soc.*, 129 (1982) 464.
13. Z. Szklarska-Smialowska, *Corros. Sci.*, 41 (1999) 1743.
14. F. Hunkeler, G. S. Frankel, H. Bohni, *Corrosion (NACE)*, 43 (1987) 189.
15. N. Sato, *Corros. Sci.*, 37 (1995) 1947.
16. S. S. A. Rehim, H. H. Hassan, M. A. Amin, *Appl. Surf. Sci.*, 187 (2002) 279.
17. S. Zein El Abedin, *J. Appl. Electrochem.*, 31 (2001) 711.
18. P. M. Natishan, E. McCafferty, G. K. Hubler, *J. Electrochem. Soc.*, 135 (1988) 321.
19. C. M. A. Brett, *J. Appl. Electrochem.*, 20 (1990) 1000.
20. N. A. Ogurtsov, A. A. Pud, P. Kamarchik, G. S. Shapoval, *Synth. Met*., 143 (2004) 43.
21. I. B. Obot1, N. O. Obi-Egbedi, *Int. J. Electrochem. Sci.*, 4 (2009) 1277.
22. A. Y. El-Etre, *Corros. Sci*., 43 (2001) 1031.
23. S. B. Saidman, J. B. Bessone, *J. Electroanal. Chem.*, 521 (2002) 87.
24. I. Lukovits, E. Kalman, F. Zucchi, *Corrosion* 57 (2001) 3.
25. I. Yamaguchi, T. Yamamoto, *React. Funct. Polymers* 61 (2004) 43.
26. E. M. Sherif, S.-M. Park, *J. Electrochim. Acta*, 51 (2006) 4665.
27. E. M. Sherif, A. A Almajid, *J. Appl. Electrochem.*, 40 (2010) 1555.
28. K. Babić-Samardžija, C. Lupu, N. Hackerman, A. R. Barron, A. Luttge, *Langmuir*, 21 (2005) 12187.

29. E. M. Sherif, A. A. Almajid, F. H. Latif, H. Junaedi, *Int. J. Electrochem. Sci.,* 6 (2011) (in press).
30. E. M. Sherif, R. M. Erasmus, J. D. Comins, *J. Colloid Interface Sci.*, 306 (2007) 96.
31. E. M. Sherif, R. M. Erasmus, J. D. Comins, *J. Colloid Interface Sci.*, 311 (2007) 144.
32. E. M. Sherif, R. M. Erasmus, J. D. Comins, *J. Electrochim. Acta*, 55 (2010) 3657.
33. E. M. Sherif, R. M. Erasmus, J. D. Comins, *J. Appl. Electrochem.*, 39 (2009) 83.
34. E. M. Sherif, R. M. Erasmus, J. D. Comins, *Corros. Sci.*, 50 (2008) 3439.
35. E. M. Sherif, S.-M. Park, *Electrochim. Acta*, 51 (2006) 6556.
36. E. M. Sherif, S.-M. Park, *Corros. Sci.*, 48 (2006) 4065.
37. E. M. Sherif, *Appl. Surf. Sci.*, 252 (2006) 8615.
38. W. J. Rudd, J. C. Scully, *Corros. Sci*., 20 (1980) 611.
39. A. Y. Musa, A. A. H. Kadhum, A. B. Muhamad, *Int. J. Electrochem. Sci.*, 5 (2010) 1911.
40. L. Vrsalovic, M. Kliškic, S. Gudic, *Int. J. Electrochem. Sci.,* 4 (2009) 1568.
41. E. M. Sherif, *J. Mater. Eng. Performance,* 19 (2010) 873.
42. E. M. Sherif, J. H. Potgieter, J. D. Comins, L. Cornish, P. A. Olubambi, C. N. Machio, *J. Appl. Electrochem.*, 39 (2009) 1385.
43. E. M. Sherif, J. H. Potgieter, J. D. Comins, L. Cornish, P. A. Olubambi, C. N. Machio, *Corros. Sci.*, 51 (2009) 1364.
44. E. M. Sherif, S.-M. Park, *J. Electrochem. Soc.*, 152 (2005) B428.
45. H. Ma, S. Chen, L. Niu, S. Zhao, S. Li, D. Li, J. Appl. Electrochem. 32 (2002) 65.